Slope stability analyses using limit equilibrium and strength reduction methods

Authors:

Zoran Berisavljević, BSc.Geol.
Koridori of Sebia
berisavljevic_zoran@yahoo.com

Dušan Berisavljević, BSc.Geol.
Institute for Materials Testing
dusan.berisavljevic@institutims.rs

Assist.Prof. **Vladimir Čebašek**, PhD.Mining
University of Belgrade
Faculty of Mining and Geology
vcebasek@rgf.bg.ac.rs

Assist.Prof. **Dragoslav Rakić** PhD.Geol.
University of Belgrade
Faculty of Mining and Geology
rgfraka@rgf.bg.ac.rs

Subject review

Zoran Berisavljević, Dušan Berisavljević, Vladimir Čebašek, Dragoslav Rakić

Slope stability analyses using limit equilibrium and strength reduction methods

This paper presents results of comparative slope stability analyses conducted by limit equilibrium and strength reduction methods. Several slopes, taken either from geotechnical practice or literature review, are considered. The influence of tension, distributed load, finite element size and model parameters is analysed in relation to the location, shape of the critical failure surface and the corresponding value of the factor of safety. Both methods provide similar results if they are correctly applied using appropriate software programs.

Key words:

limit equilibrium, reduction of strength parameters, dilatancy, optimisation, Bezier curve, tension zone

Pregledni rad

Zoran Berisavljević, Dušan Berisavljević, Vladimir Čebašek, Dragoslav Rakić

Analize stabilnosti pokosa metodama granične ravnoteže i smanjenja parametara čvrstoće

U ovom su radu predstavljeni rezultati usporedne analize stabilnosti pokosa metodama granične ravnoteže i smanjenja parametara čvrstoće tla. Razmatrano je nekoliko pokosa uzetih iz literature ili iz geotehničke prakse. Analiziran je utjecaj vlačnog naprezanja, raspodijeljenog opterećenja, veličina konačnog elementa i parametri modela na lokaciji te oblik kritičnog loma i odgovarajuće vrijednosti faktora sigurnosti. Obje navedene metode daju slične rezultate ako se ispravno primijene u odgovarajućim računalnim programima.

Ključne riječi:

granična ravnoteža, smanjenje parametara čvrstoće, dilatancija, optimizacija, Bézierova krivulja, vlačna zona

Übersichtsarbeit

Zoran Berisavljević, Dušan Berisavljević, Vladimir Čebašek, Dragoslav Rakić

Stabilitätsanalyse von Böschungen mittels Methoden des Grenzgleichgewichts und der Abminderung von Festigkeitsparametern

In dieser Arbeit werden Resultate der Stabilitätsanalyse von Böschungen mittels der Methoden des Grenzgleichgewichts und der Abminderung von Festigkeitsparametern verglichen. Es werden sowohl aus der Literatur übernommene, als auch praktische geotechnische Beispiele erläutert. Dabei werden der Einfluss von Zugspannungen, verteilten Lasten, Dimensionen finiter Elemente und lokalen Modelparametern analysiert, sowie Bruchformen und entsprechende Werte der Sicherheitskoeffizienten dargestellt. Beide untersuchten Methoden ergeben ähnliche Resultate, wenn sie mittels entsprechender Computerprogramme korrekt angewandt werden.

Schlüsselwörter:

Grenzgleichgewicht, Abminderung von Festigkeitsparametern, Dilatation, Optimierung, Bézier-Kurve, Zugzone

Zoran Berisavljević, Dušan Berisavljević, Vladimir Čebašek, Dragoslav Rakić

1. Introduction

In the engineering practice, slope stability analyses are most commonly performed using limit equilibrium methods (LEM). The most widely used are the methods of slices, where the soil mass above an assumed failure surface is divided into several, usually vertical, slices and, as a result, the value of the factor of safety is obtained:

$$Fs = \frac{\tau_f}{\tau_m} \qquad (1)$$

where τ_f is the actual available shear strength of the material, and τ_m is the mobilised shear strength or the average shear stress on the hypothetical failure surface mobilized to maintain the body in equilibrium. Despite their inherent weaknesses [1-3], these methods have been developed and tested by means of actual case histories. In order to render the analysis statically determinate, some assumptions must be made. The assumption is made that the interslice shear force X is related to the interslice normal force E (total or effective), by mathematical expression:

$$X = \lambda f(x)E \qquad (2)$$

where λ is the scaling constant representing the percentage of the function $f(x)$ used for solving for the factor of safety equation, and $f(x)$ is the functional relationship (interslice force function) that describes the manner in which the magnitude of X/E varies across the failure surface.

The final result is usually not very sensitive to the choice of $f(x)$ function [4-6], but examples where the solution is very sensitive to the assumed interslice force function have also been reported in the literature, e.g. by Krahn [2]. Although limit equilibrium methods adopt the general philosophy of an upper bound solution [7], they do not meet all accuracy requirements. Izbicki [8] defined the results of limit equilibrium methods as a "reduced" upper bound, implying that the LEM factor of safety will be slightly lower than the upper bound factor of safety.

Bishop's simplified method [9] is used to calculate the factor of safety of a circular failure surface, which has proven to provide the results similar to those obtained with some more rigorous formulations. As to the methods that satisfy all static equilibrium elements, the Maksimovic's method (1979), Spencer method (1967) and GLE method (Fredlund and Krahn, 1977) are used. The position and shape of the critical failure surface is determined by the use of the semi and fully automatic search techniques. The interactive optimization algorithm implemented in the software package BGSLOPE [10, 11] is used to obtain the critical failure surface described by Bezier or a polygonal curve. This procedure is found to be the most versatile for comparison with the finite element method results, as it gives the user the possibility to successively manage the movements of control points of Bezier polygon or coordinate points of a polygonal curve. The analyses in LEM are performed by assuming the linear Mohr-Coulomb failure criterion. In this way, the input of no more than three parameters is needed, namely the total unit weight of material (γ), cohesion (c), and angle of shearing resistance (φ).

The finite element method (FEM) is a numerical technique for finding approximate solutions to boundary value problems for partial differential equations. It theoretically satisfies all requirements that must be met for a complete solution to a slope stability problem [12]. The material behaviour in FEM is described by an elastic, perfectly plastic model complying with the Mohr-Coulomb failure criterion [13]. This model takes into account shear strength and deformation parameters. Three additional parameters, along with the aforementioned ones, are the modulus of elasticity, E, Poisson's ratio, ν, and angle of dilatancy, ψ. Several authors [14-16] have shown that the deformation parameters E and ν, as well as the domain size, have an insignificant influence on the factor of safety value. The effect of dilatancy on the final result has also been investigated by several authors [16, 17], and is re-analysed in this paper. In case of non-associated plasticity, the positive angle of dilatancy is calculated based on a simple, widely accepted, relationship ($\psi = \varphi - 30°$). In the case of $\varphi \leq 30°$, the value of ψ equals to $0°$. Exceptionally, in the example No. 4, the angle of dilatancy is assumed to be the difference between the Coulomb angle and the basic angle used in the hyperbolic description of the non-linear failure envelope [18-20]. There are two commonly used definitions of the factor of safety in FEM, namely the strength reserving definition, and the overloading definition [21-23]. The location of the critical failure surface, as well as the factor of safety, is dependent on the chosen definition. In this paper, the value of the factor of safety is determined based on the strength reduction method (SRM), where the soil strength is artificially weakened until the slope fails. Numerically, this occurs when it is no longer possible to obtain a converged solution. This can be expressed by the equation:

$$SRF = \frac{\tan \varphi}{\tan \varphi_m} = \frac{c}{c_m} \qquad (3)$$

where SRF is the total multiplier (strength reduction factor) that is used to define the value of soil strength parameters at a given stage of the analysis, c, φ are input values of shear strength parameters, and c_m, φ_m are mobilized or reduced values used in the analysis.

At the start of a calculation, SRF is set to 1.0, i.e. all material strengths are set to their input values. In the state of failure, the SRF defined by eqn. (3) corresponds to the value of the factor of safety given in eqn. (1). In FEM, no assumption needs to be made about the shape or location of the failure surface. Failure occurs through the zones within the soil mass in which the soil shear strength is unable to resist the applied shear stress [15]. All calculations are performed in static drained conditions assuming effective shear strength and deformation parameters, without considering seismic effects. The influence of groundwater level and distributed load is examined.

Various investigations [14, 24, 25] showed that it cannot be readily concluded which method gives the higher value of the factor of safety, as the analysis is dependent on the specific problem and software package used in the analysis. In order to investigate the influence the implemented numerical algorithm exerts on the final result, certain analyses have been performed using four commercial software packages. BGSLOPE and Slide are based on the limit equilibrium method, whereas Plaxis and Phase[2] are based on the finite element method. For comparison purposes, the shapes of critical failure surfaces are overlaid on the Plaxis finite element model.

2. Examples of comparative analyses

2.1. Example 1: Side slope of the Beli potok tunnel on the Belgrade Bypass

According to the design [26], the side slopes of the cut and cover part of the Beli potok tunnel are 19 m high, with 1/2 inclination (v/h), and one berm at mid-height of the slope 5 m in width. The ground profile is composed of six horizontal layers, as shown in Figure 1.
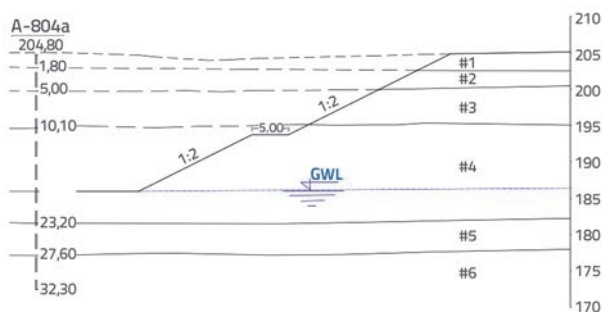

Figure 1. Typical cross-section of side slope

Based on the monitoring of piezometer constructions, the groundwater level is situated at the depth of 18 m. Triaxial CU tests results (with pore pressure measurements), simple shear and oedometer results, and extensive in situ (CPT) measurements, were used to derive shear strength and deformation parameters. The parameters used for the analyses are summarized in Table 1.

For layers #3 and #4, laboratory tests showed variation of the cohesion and angle of shear resistance values, and so the analyses were performed for two different sets of parameters. The BGSLOPE software was used to compute the factor of safety by means of limit equilibrium methods. In order to obtain the critical failure surface, seven control points of the smooth Bezier curve were successively moved in various directions, in 0.05 m increments, until the smallest factor of safety was obtained. The smallest factor of safety was calculated by assuming the half-sine interslice force function. In order to eliminate tension in the upper part of the slope, the tension crack consistent with the factor of safety was introduced. The influence of tension will be discussed in more detail in example No. 3. The Plaxis software was used to compute the factor of safety with SRM. The finite element model consists of 3011 15-noded triangular elements automatically generated based on a robust triangulation procedure. An average element size was 1.168 m. The critical failure surfaces are compared and shown in Figure 2. The values of the factors of safety are summarized in Table 2.
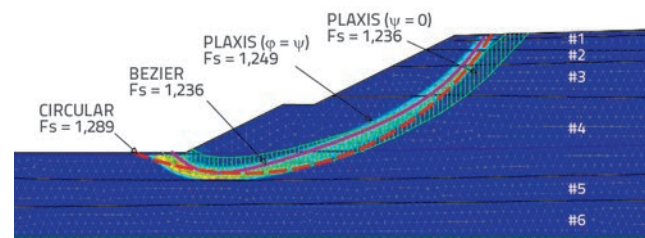

Figure 2. Results of analyses

Table 2. Calculation results

Method	Safety factor (figure 2)	Safety factor (figure 3[a])
BGSLOPE (Bishop)	1.289	1.181
BGSLOPE (Maksimovic, optimized)	1.236	1.137
Plaxis ($\varphi = \psi$)	1.249	1.153
Plaxis ($\psi = 0$)	1.236	1.128

[a]Only the smallest factors of safety are presented

Table 1. Input parameters for analyses

Parameters	Parameter marker	#1	#2	#3	#4	#5	#6
Unit weight, [kN/m³]	γ/γ_z	19	18	18.5	19/20	19	20
Young's modulus, [kN/m²]	E	18750	7430	8900	18750	22300	22300
Poisson's ratio, [-]	ν	0.3	0.3	0.3	0.3	0.3	0.3
Cohesion, [kN/m²]	c	5	10	15/**10***	10/**5***	5	5
Angle of shear resistance, [°]	φ	24	18	18/**17***	20/**21***	24	24
Angle of dilatancy, [°]	ψ	24/0	18/0	18/0	20/0	24/0	24/0

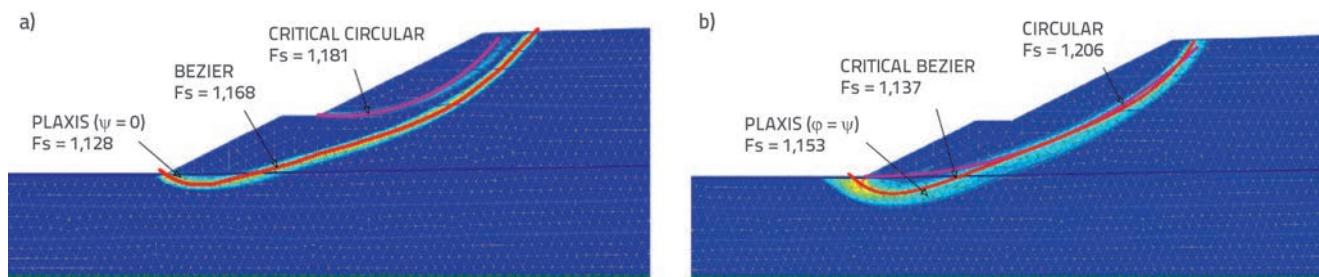*Values of shear strength parameters c i φ correspond to an analysis shown in Figure 3*

Figure 3. Various failure surfaces: a) Plaxis ($\psi = 0°$), critical circular and Bezier; b) Plaxis ($\varphi = \psi$), circular and critical Bezier

As shown in Figure 2, the optimized critical failure surface obtained by LEM corresponds well with the finite element solution in case of the associated flow rule ($\varphi = \psi$). The same safety factors were obtained for Plaxis ($\psi = 0°$) and an optimized Bezier curve. The critical circular failure surface overestimates the value of the factor of safety by 4.3 %.

Safety factor values obtained with the second set of parameters are shown in Table 2, while shapes of failure surfaces are given in Figure 3. The critical circular failure surface is located at the upper part of the slope, overestimating the factor of safety by 3.9-4.3 %. The critical failure surface in Plaxis is obtained for $\psi = 0°$ and amounts to Fs = 1.128. It extends throughout the entire height of the slope. The critical LEM failure surface amounts to Fs = 1.137, and its position corresponds to the Plaxis $\varphi = \psi$ solution. If the Bezier curve is optimized to have the same shape as the Plaxis $\psi = 0°$ ° solution, a local minimum is obtained. If the smallest factors of safety are compared by the two methods, it can be seen that their difference is insignificant and amounts to 0.8 %. The smallest factor of safety of the circular failure surface that extends from the crest to the toe of the slope is Fs = 1.206.

2.2. Example 2: embankment widening on M-19 road

The side embankment, approx. 8 m in height, is to be constructed for the widening of the existing road M-19 on Belgrade-Ljig section (approximately at KM 4+100). The design proposed several alternative solutions as elaborated in [27]. Only the solution with the lightweight fly-ash material is analysed in this paper. The slope geometry is shown in Figure 4.
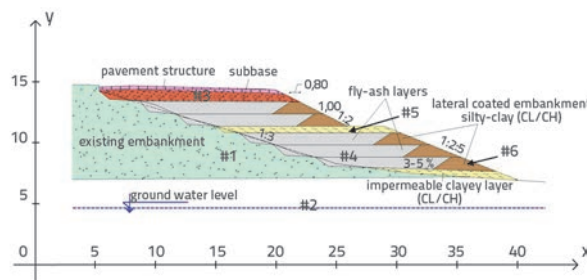

Figure 4. Road embankment widening using fly-ash material

Soil parameters used in the analyses are derived from field investigations and laboratory testing, cf. Table 3. Shear strength parameters for fly-ash were determined by direct shear testing on compacted samples (according to Proctor test), consolidated for 42 hours [28]. It is important to note that fly-ash exhibits pozzolanic activity, i.e. it has the self-binding ability due to chemical reaction with calcium hydroxide in the presence of water. This leads to an increase in shear strength during compaction and consolidation processes. The linear Mohr-Coulomb envelope was defined for the normal stress level of up to 150 kN/m^2. Young's modulus was determined by correlation with the previously determined oedometer modulus (on compacted samples) [28] according to the theory of elasticity with the Poisson's ratio assumed to be equal to 0.3.

The BGSLOPE software was used to perform LEM analyses. Linear distribution of the interslice force function is assumed along the optimized Bezier curve. This distribution is defined by specifying one parameter ($z_1 = 0.1$), on the x-axis along failure surface, whereas one additional value of parameter

Table 3. Input parameters for analyses

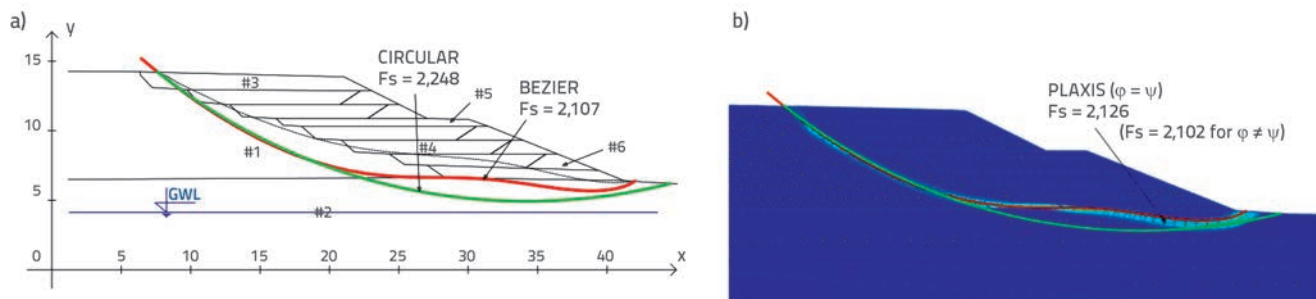| Parameters	Parameter marker	#1	#2	#3	#4	#5/#6
Unit weight, [kN/m^3]	γ/γ_z	18	18/19	18.5/20	8.5	18
Young's modulus, [kN/m^2]	E	18750	6300	26000	24500	18750
Poisson's ratio, [-]	ν	0.3	0.3	0.3	0.3	0.3
Cohesion, [kN/m^2]	c	10	2	1	12	5
Angle of shear resistance, [°]	φ	15	25	34	54	25
Angle of dilatancy, [°]	ψ	15/0	25/0	34/4	54/24	25/0

Figure 5. Results of analyses: a) LEM; b) LEM surfaces overlaid on a finite element model

z is assumed to be equal to 1, at the middle of the failure surface. The finite element model in Plaxis is defined by 1716 15-noded triangular elements. An average element size is 0.942 m. Critical failure surfaces overlap, as shown in Figure 5. The corresponding factors of safety are summarized in Table 4.

Table 4. Calculation results

Metoda	Fs
BGSLOPE (Bishop)	2,248
BGSLOPE (Maksimovic, optimized)	2,107
Plaxis ($\varphi = \psi$)	2,126
Plaxis ($\varphi \neq \psi$)	2,102

As can be seen in Figure 5, the location of the critical failure surface obtained by Plaxis ($\varphi = \psi$) corresponds to the LEM solution, whereas the difference between the factors of safety obtained by Plaxis ($\varphi \neq \psi$) and LEM is insignificant. The critical circular failure surface overestimates the factor of safety by 6.7 %. The influence of load distribution on the final result is analysed in the following two examples. The occurrence of tension on top of the slope (with horizontal surface) is also discussed.

2.3. Example no. 3: NTNU slope

This relatively simple slope was analysed as a part of PhD thesis defended at Norwegian University of Science and Technology. In this study [17], the software package Slope/W with Morgenstern-Price method was used to perform the LEM analyses. Tension was not considered.
In order to inspect the findings, an example is re-analysed. The model consists of a two-layered slope, as shown

in Figure 6. Parameters used to perform the analyses are summarized in Table 5. The BGSLOPE (Maksimovic's method) and Slide (GLE method) software are used to compute the LEM factor of safety. The half-sine interslice force function is assumed in calculations. The Plaxis and Phase² are used to obtain the SRM factor of safety. The calculation model used in Plaxis consists of 2249 15-noded triangular finite elements. An average element size is 0.516 m. Phase² model is represented by 7433 6-noded triangular finite elements.
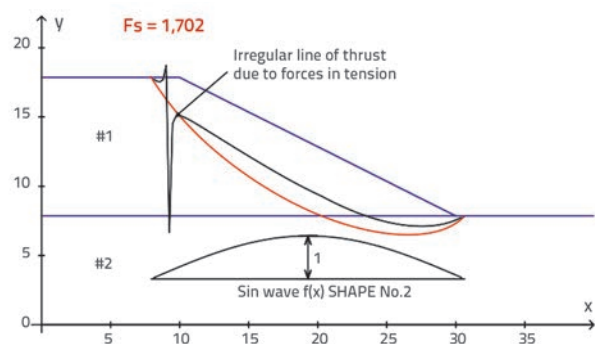

Figure 6. Slope geometry and appearance of tension (BGSLOPE calculations)

In the limit equilibrium calculations, the tension occurred in the upper part of the slope due to cohesion term in the soil strength description of layer #1, as shown in Figure 6. The tension is indicated as irregularity in the line of thrust, which appears outside the sliding body, rendering the solution physically inadmissible. As a result of tension, normal forces at bases of the slices and interslice forces are negative, meaning that the slices are in a state of buoyancy although in reality there will be no tendency for the mass to lift upwards. It was also established that the presence of negative forces could lead to numerical instability

Table 5. Input parameters for analyses

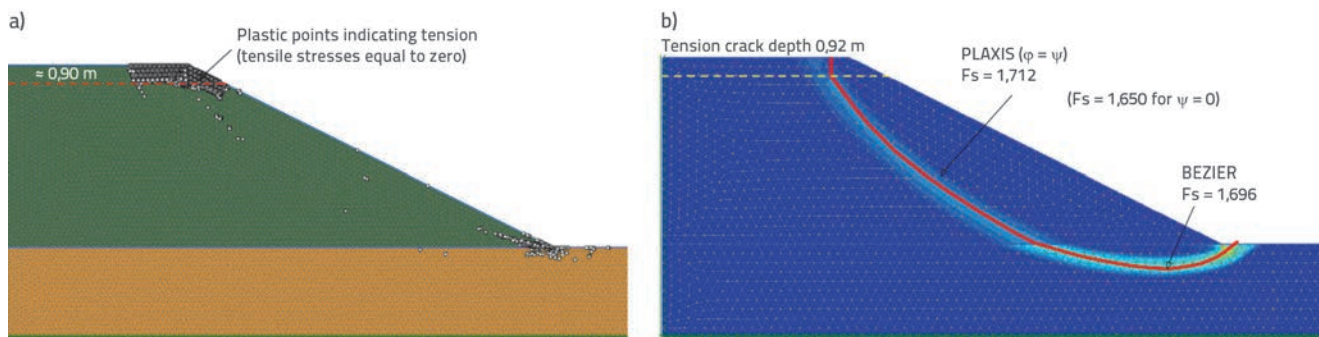| Parameter / Layer	Unit weight γ [kN/m³]	Young's modulus E [kN/m²]	Poisson's ratio ν [-]	Cohesion c [kN/m²]	Angle of shear resist. φ [°]	Angle of dilatancy ψ (°)
#1	18	5000	0.3	10	30	30/0
#2	18	5000	0.3	5	25	25/0

Figure 7. Results of the analyses: a) distribution of plastic points; b) factor of safety values

when computing the factor of safety [1, 11]. In order to avoid this, Spencer [29, 30] suggested that a tension crack zone should be introduced at the top of the slope. The depth of the tension zone was assumed to be equal to the depth of the zero active effective stress, consistent with the factor of safety of the slope:

$$Hc = \frac{2c}{\gamma Fs(1-r_u)} \; tan(45+\varphi/2) \qquad (4)$$

where r_u is the pore pressure ratio, and H_c is the depth to the zero active effective stress.

In order to make FEM results comparable with LEM values, a zero tensile strength is assigned to all materials in FEM [25, 31]. After a number of trials, it was concluded that the depth of the tension point zone is in good agreement with the depth calculated according to eqn. (4), for the ordinary combinations of strength parameters. The deformation parameters E and ν do not have any influence on the tension zone depth. The angle of dilatancy increases the factor of safety, thus decreasing the depth of the tension zone. These findings are valid for a fully developed failure mechanism. The location of the critical failure surface given in Plaxis ($\varphi = \psi$) corresponds to the BGSLOPE solution, as shown in Figure 7b.

Table 6. Calculation results

Metoda	Fs	Fs accord. [17]	Fs (for load 92 kPa)
Slope/W (Bishop)		1.737	
Slope/W(M-P, optimized)		1.701[a]	
Slide (GLE, optimized)	1.691		1.386
BGSLOPE (Maksimovic, optimized)	1.696 (1.702)[a]		1.387
Plaxis ($\varphi = \psi$)	1.712		1.402
Plaxis ($\psi = 0$)	1.650	1.654	1.334
Phase[2] ($\psi = 0$)	1.690		
[a]without tension crack			

Failure mechanisms obtained from Phase[2] and Slide are identical to the Plaxis and BGSLOPE calculations, respectively, and are thus not included in Figure 7. The corresponding factors of safety are summarized in Table 6.

The calculated tension crack depth of 0.92 m is in good agreement with the depth of the tension zone obtained by Plaxis, as shown in Figure 7a. If compared to the Plaxis ($\psi = 0°$) solution, the critical failure circle overestimates the value of the factor of safety by 5 % and only by 2.7 % if compared to the Phase[2] ($\psi = 0°$) results.

In order to investigate the influence of distributed load on the stability of the slope, an arbitrary chosen value of 92 kPa is assumed to act on the top of the slope, as shown in Figure 8.
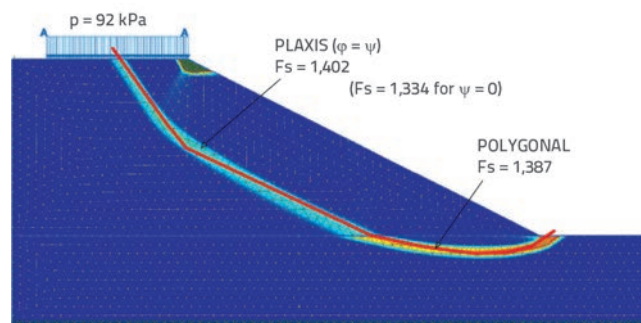

Figure 8. Influence of distributed load

The effect of distributed load eliminates the tension. Calculation results are summarized in Table 6. The failure surface in Plaxis shows sharp transition in the upper part of the slope due to formation of the active Rankine zone. The smallest factor of safety is obtained in BGSLOPE by optimization of the polygonal failure surface defined by nine points. The value of Fs = 1.387 is by 4 % higher than the value obtained by Plaxis for an assumed non-dilatant material behaviour. The shape of the polygonal failure surface corresponds well to the Plaxis solution, as shown in Figure 8. The same critical failure surface is obtained from Slide (GLE method) with the corresponding factor of safety, Fs = 1.386, which is practically the same value as the one computed in BGSLOPE.

2.4. Example 4: New Valley Project - stability of rock slopes

This example examines stability of the rock slope formed for construction of the foundation pit for the pumping station in the scope of the "New Valley Project" in Egypt. Plaxis calculations performed for software verification [20] were re-analysed by introducing different mesh coarseness values. A typical cross-section is shown in Figure 9. The slope, 1.2:1 (v:h), is approx. 50 m high with two intermediate berms 10 m in width. The parameters used in calculations are
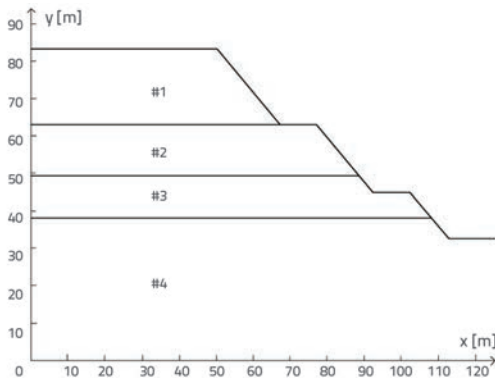

Figure 10. Results of analyses a) tension zone depth; b) shape and position of failure surfaces

Figure 9. Typical cross-section of rock slope

summarized in Table 7. The analyses were performed assuming dry slope conditions.

FEM results are presented for the model with 3459 15-noded triangular finite elements, with an average element size of 1.740 m. LEM calculations were performed with the software package Slide (GLE method). The interslice force function $f(x)$ was assumed to have linear distribution defined along the horizontal axis by two parameters ($z_1 = 0.4$ and $z_2 = 2$) at the opposite sides of the failure surface. The location of the critical failure surface was found, as in the preceding example, by an automatic search technique based on the Monte Carlo method. Calculation results are shown in Figure 10, and safety factors values are summarized in Table 8. The second analysis considered the case with distributed loads acting on the top of the slope. Calculation results are shown in Figure 11, and the corresponding factors of safety are summarized in Table 8.

As shown in Figure 11, the locations of critical failure surfaces and corresponding factors of safety are in good agreement. If Figures 10 and 11 are compared, it can be concluded that failure zones are shifted towards the back of the slope and safety factors are reduced to Fs = 1.723 (1.729) when the load is applied. Additional analyses were performed in order to check the influence of the finite element size on the factor of safety. Calculation results for meshes consisting of 64 to 11064 finite elements are shown in Figure 12. The factor of safety varies between 1.973 (64 elements) and 1.880 (11064 elements). Further refinement would lead to an insignificant decrease in the factor of safety, but the computation time would increase dramatically. In order to reduce the computation time, one can locally refine regions that are of

Table 7. Input parameters for analyses

Parameter	Parameter marker	#1	#2	#3	#4
Unit weight [kN/m³]	γ	22	22.4	21.9	21.6
Shear modulus [kN/m²]	G	2.400.000	4.200.000	2.000.000	2.000.000
Poisson's ratio [-]	v	0.35	0.32	0.4	0.32
Cohesion. [kN/m²]	c	100	135	55	70
Angle of shear resist. [°]	φ	44	52	28	38
Angle of dilatancy. [°]	ψ	44/14	52/22	28/4	38/9

Table 8. Calculation results

Method	Fs	Fs accord. [20]	Fs (for load 150 and 500 kPa)
BGSLOPE (Bishop)		2.057	
BGSLOPE (Maksimovic. optimized)		1.951	
Slide (GLE. optimized)	1.879		1.729
Plaxis ($\varphi = \psi$)	1.900	1.967	1.757
Plaxis ($\psi \neq \varphi$)	1.884	1.927	1.723

more interest from the stability point of view, and keep coarser mesh closer to the far end of the model.
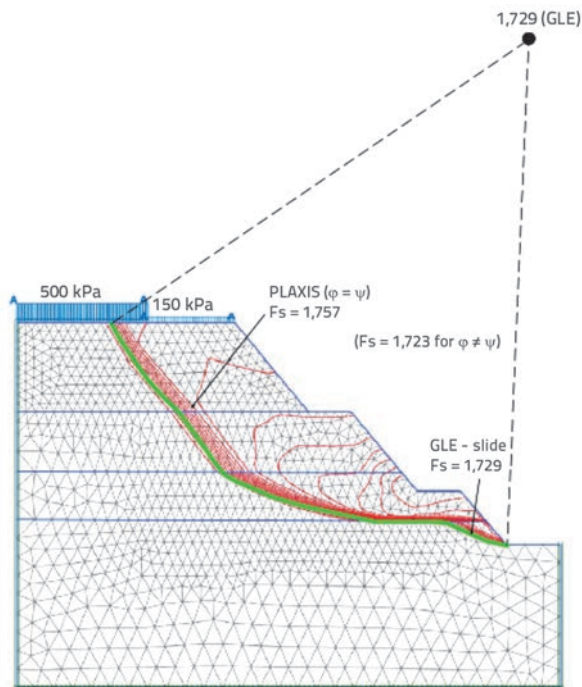

Figure 11. Analysis for varying distribution of load
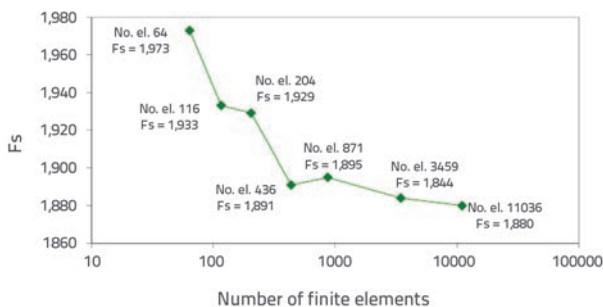

Figure 12. Factor of safety vs mesh coarseness

3. Conclusions

The comparative study was performed in order to investigate the applicability of FEM and LEM to calculate the smallest factor of safety and location of the critical failure surface. The influence of different parameters on the final result was investigated. In the presented examples, the critical circular failure surface overestimates the factor of safety by up to 9 %. Cheng [32] gives a comprehensive review about the problems associated

with the possibility of locating the critical failure surface in the LEM. The fully automatic optimization could sometimes lead to the solution corresponding to a local minimum. For this reason, the semi-automatic search technique, such as an interactive optimization algorithm, is suggested for finding the location of the critical failure surface. The smooth Bezier curve is in most cases more suitable for calculating the smallest factor of safety than the polygonal curve. However, sharp transitions, as in the case of distributed load acting at the top of the slope, are more readily described by polygonal curve. The shape of the interslice force function f(x) should be chosen so as to obtain the smallest factor of safety. Satisfactory results are obtained by commonly used distributions like Spencer, half-sine, or linear.

It is commonly accepted that the values E and ν and the domain size do not have any (or have a very small) influence on the factor of safety and the location of the critical failure surface in SRM. If realistic values of E and ν (determined by laboratory or in situ tests) are used, the results should be in close agreement with LEM results. Cheng et al. [14] show that the greater differences between the two methods could be expected in a special case of the slope with a thin soft band. Despite the generally low confinement environment, the angle of dilatancy exerts some influence on the SRM results. If the associated flow rule is assumed in SRM, the locations of critical failure surfaces obtained by the two methods are virtually the same. However, the best prediction of the factor of safety value compared to LEM is obtained for the non-associated flow rule, in case realistic values of positive dilatancy are incorporated into analysis [33, 34]. If, for example, the non-dilatant material behaviour is assumed in the first case given in example No. 4, the value of the factor of safety is 1.796. In case of the associated flow rule, this value is by 6 % higher. Another parameter influencing the SRM results is the finite element size. It is suggested that the analysis should be performed with the local mesh refinement, so that the time required for calculation is acceptable from the practical point of view. The advantage is given to the 15-noded over the 6-noded triangular finite elements. If zero tensile stresses are assumed in the tension cut-off option in Plaxis, a good correspondence is observed between the tension crack depth given in eqn. (4), and the distribution of plastic tension points.

Different numerical algorithms implemented in software packages such as Plaxis, Phase², Slide, and BGSLOPE, and the varying choice of the number of allowed iterations, tolerance, number of slices, etc. have an influence on the final result in both FEM and LEM. From the practical point of view, both methods provide similar results If correctly applied with all available software options.

REFERENCES

[1] Ching, R.K.H., Fredlund, D.G.: Some difficulties associated with the limit equilibrium method of slices, *Canadian Geotechnical Journal*, 20 (1983), pp. 661-672, http://dx.doi.org/10.1139/t83-074

[2] Krahn, J.: The 2001 R.M. Hardy Lecture: The limits of limit equilibrium analyses, *Canadian Geotechnical Journal*, 40 (2003), pp. 643-660, http://dx.doi.org/10.1139/t03-024

[3] Krahn, J.: Limit Equilibrium, Strength Summation and Strength Reduction Methods for Assessing Slope stability, *Proc. of the 1st Canada-U.S. Rock Mechanics Symposium*, Vancouver, 2007.

[4] Duncan, J.M.: State of the art: limit equilibrium and φinite-element analysis of slopes, *Journal of Geotechnical and Geoenvironmental Engineering ASCE*, 122 (1996) 7, 577-596.

[5] Fredlund, D.G.: State of the Art Lecture-Analytical methods for slope stability analysis, *IV Int. Symposium on Landslides*, Toronto, 1984.

[6] Maksimovic, M.: *Soil mechanics (in Serbian)*, Gradjevinska knjiga, Belgrade, 2005.

[7] Chowdhury, R. with contributors: Flentje, P., Bhattacharya G.: *Geotechnical slope analysis*, CRC Press/Balkema, London, 2009.

[8] Izbicki, R.: Limit plasticity approach to slope stability problems, *Journal of Geotechnical and Geoenvironmental Engineering ASCE*, 107, (1981), GT2, pp. 228-233.

[9] Bishop, A.W.: The use of slip circle in the stability analysis of slopes, Geotechnique, 5 (1955), pp. 7-17, http://dx.doi.org/10.1680/geot.1955.5.1.7

[10] Maksimovic, M.: General slope stability software package for micro-computers, *6th Int. Conf. on Numerical Methods in Geomechanics*, Innsbruck, pp. 2145-2150, 1988.

[11] Maksimovic, M.: *BGSLOPE 11-A, Slope Stability for PC*, User's manual, 2011.

[12] Potts, D.M., Zdravkovic, L.: *Finite element analysis in geotechnical engineering: theory*, Thomas Telford, London, 1999., http://dx.doi.org/10.1680/feaiget.27534

[13] Brinkgreve, R.B.J., Bakker, H.L.: Non-linear finite element analysis of safety factors, *Proc. of the 7th Int. Conf. on Comp. Methods and Advances in Geomechanics (IACMAG)*, Cairns, pp. 1117-1122, 1991.

[14] Cheng, Y.M., Lansivaara, T., Wei, W.B.: Two-dimensional slope stability analysis by limit equilibrium and strength reduction methods, *Computers and Geotechnics*, 34, (2007), pp. 137-150, http://dx.doi.org/10.1016/j.compgeo.2006.10.011

[15] Griffiths, D.V., Lane, P.A.: Slope stability analysis by finite elements, *Geotechnique*, 49 (1999) 3, pp. 378-403.

[16] Hammah, R., Jacoub, T., Corkum, B., Curran, J.: A comparison of finite element slope stability analysis with conventional limit-equilibrium investigations, *Rocscience*, (2005).

[17] Aryal, P.A.: *Slope Stability Evaluations by Limit Equilibrium and Finite Element Methods*, PhD thesis, NTNU, University of Trondheim, Norway, 2006.

[18] Maksimovic, M.: Limit equilibrium for nonlinear failure envelope and arbitrary slip surface, *Proc. 3rd Int. Conf. on Numerical Methods in Geomechanics*, Aachen, pp. 769-777, 1979.

[19] Maksimovic, M.: A Family of Nonlinear Failure Envelopes for Non-cemented Soils and Rock Discontinuities, *Electronic Journal of Geotechnical Engineering*, 1 (1996), pp. 1-62.

[20] Verification for BGSLOPE software: New valley project - Stability of rock slopes, Report No. 2.

[21] Farias, M.M., Naylor, D.J.: Safety analysis using finite element, *Computers and Geotechnics*, (1988) 22(2), pp. 165-181, http://dx.doi.org/10.1016/S0266-352X(98)00005-6

[22] Zheng, H., Tham, L.G., Liu, D.F.: On two definitions of the factor of safety commonly used in the finite element slope stability analysis, *Computers and Geotechnics*, 33 (2006), pp.188-195, http://dx.doi.org/10.1016/j.compgeo.2006.03.007

[23] Zheng, H., Sun, G., Liu, D.F.: A practical procedure for searching critical slip surfaces of slopes based on the strength reduction technique, *Computers and Geotechnics*, 36 (2009), pp.1-5, http://dx.doi.org/10.1016/j.compgeo.2008.06.002

[24] Alkasawneh, W., Husein Malkawi, A.I., Nusairat, J.H.: A comparative study of various commercially available programs in slope stability analysis, *Computers and Geotechnics*, 35 (2008), pp. 428-435, http://dx.doi.org/10.1016/j.compgeo.2007.06.009

[25] Bojorque, J., De Roeck, G., Maertens, J.: Comments on 'Two-dimensional slope stability analysis by limit equilibrium and strength reduction methods by Y. M. Cheng, T. Lansivaara and W. B. Wei [Computers and Geotechnics 2007; 34:137-150']', *Computers and Geotechnics*, 35 (2008), pp. 305-308, http://dx.doi.org/10.1016/j.compgeo.2007.04.005

[26] The Highway Institute: *Project documentation*, (2011).

[27] Berisavljevic, Z.: Problems in predicting the behaviour of the road embankment built on a soft soil, *Proc. of the 20th EYGEC*, Brno, pp. 242-247, 2010.

[28] The Highway Institute: Research-developmental project - *Utilization of fly-ash and slag produced in thermo-electric power plants 'Nikola Tesla A& B' and 'Kostolac A & B' for road construction*, Belgrade, 2008, pp.157.

[29] Spencer, E.: Effect of tension on stability on embankments. *Journal of Geotechnical and Geoenvironmental Engineering ASCE*, 94, (1968), SM5, pp.1159-1173.

[30] Spencer, E.: Thrust line criterion in embankment stability analysis. *Geotechnique*, (1973) 23, pp. 85-100, http://dx.doi.org/10.1680/geot.1973.23.1.85

[31] Plaxisbv.: *Finite Element Code for Soil and Rock Analysis, Slope Stability Analysis*, Delft University of Technology and Plaxis, The Netherlands.

[32] Cheng, Y.M.: Location of critical failure surface and some further studies on slope stability analysis. *Computers and Geotechnics* 30 (2003), pp. 255-267, http://dx.doi.org/10.1016/S0266-352X(03)00012-0

[33] Davis, R.O., Selvadurai, A.P.S.: *Plasticity and geomechanics*, Cambridge University press, New York, 2002., http://dx.doi.org/10.1017/CBO9780511614958

[34] Vermeer, P.A., de Borst, R.: *Non-associated plasticity for soils, concrete and rock* 29(3), Heron, Delft, 1984.